Roles of the Methane Monooxygenase Reductase Component in the Regulation of Catalysis†

Yi Liu,‡,§,|| Jeremy C. Nesheim,‡,§ Kim E. Paulsen,§,⊥,# Marian T. Stankovich,*,§,⊥ and John D. Lipscomb*,‡,§

Departments of Biochemistry and Chemistry, and Center for Metals in Biocatalysis, University of Minnesota, Minneapolis, Minnesota 55455

Received November 4, 1996; Revised Manuscript Received February 18, 1997⊗

ABSTRACT: The reductase component (MMOR) of the soluble methane monooxygenase isolated from *Methylosinus trichosporium* OB3b catalyzes transfer of $2e^-$ from NADH to the hydroxylase component (MMOH) where oxygen activation and substrate oxidation occur. It is shown here that MMOR can also exert regulatory effects on catalysis by binding to MMOH or to the binary complex of MMOH and component B (MMOB), another regulatory protein. MMOR alters the oxidation−reduction potentials of the dinuclear iron cluster at the active site of MMOH. Although little change is observed in the potential for the first electron transfer to the cluster ($E_1°' = 76$ mV), the $E_2°'$ potential value for the second electron transfer is increased from 21 to 125 mV. This shift provides a larger driving force for electron transfer from MMOR and favors transfer of two rather than one electron as required by catalysis. Similar positive shifts in potential are observed even in the presence of MMOB which has been shown to cause a 132 mV negative shift in the midpoint potential of MMOH in the absence of MMOR. MMOR is also shown to decrease the rate of reaction between the fully reduced MMOH−MMOB and O_2 approximately 20-fold at 4 °C. However, the time course of the key catalytic cycle intermediate that can react with substates, compound Q, is unaffected. This implies a compensating faster decay of one or more of the intermediates that occur between diferrous MMOH and compound Q in the reaction cycle, thereby limiting potential nonproductive autodecay of these intermediates. Accordingly, an increase in single turnover product yield is observed in the presence of MMOR. Interestingly, MMOR can cause the redox potential increases, changes in rates, and the increase in product yield when present at only 10% of the concentration of MMOH active sites. Substrate binding is shown to induce negligible changes in the redox potentials. Two alternative regulatory schemes are presented based on (i) thermodynamic coupling of component binding and redox changes or (ii) dynamic interconversion of two states of MMOH promoted by MMOR.

Efficient catalysis of methane oxidation by the soluble form of methane monooxygenase (MMO)[1] isolated from *Methylosinus trichosporium* OB3b requires a complex of three protein components: a 245 kDa hydroxylase (MMOH) containing an oxygen-bridged dinuclear iron cluster in each protomer of the $(\alpha,\beta,\gamma)_2$ structure, a 38 kDa reductase containing FAD and a [2Fe-2S] cluster (MMOR), and a cofactorless 15 kDa "B" component (MMOB) (Dalton, 1980; Lipscomb, 1994; Wallar & Lipscomb, 1996).

$$CH_4 + O_2 + NADH + H^+ \xrightarrow{\text{MMOR·MMOB·MMOH}} CH_3OH + H_2O + NAD^+ \quad (1)$$

The active site of oxygen activation and substrate oxidation is associated with the dinuclear iron cluster of MMOH (Fox et al., 1989; Rosenzweig et al., 1993, 1995; Elango et al., 1997). This cluster can be stabilized in three different oxidation states: an Fe(III)Fe(III) resting state, an unreactive mixed valence Fe(III)Fe(II) state, and the reduced Fe(II)Fe(II) diferrous state which reacts with O_2 to initiate the catalytic cycle. All three states are virtually colorless; however, distinct EPR signals arise from each state (Fox et al., 1988, 1993; Hendrich et al., 1990). If the diferric diiron cluster of MMOH is chemically reduced to the diferrous state and then exposed to O_2 and a hydrocarbon substrate, it will turnover once in the absence of MMOB and MMOR to yield water and the oxidized hydrocarbon, with a yield of ∼40% (Fox et al., 1989; Liu, Y., et al., 1995). However, under physiological conditions, no turnover coupled to NADH

† The work was supported by NIH Grants GM40466 to J.D.L. and GM29344 to M.T.S. J.C.N. was supported in part by NIH Training Grant GM08277.

* Authors to whom correspondence should be addressed. J.D.L.: Department of Biochemistry, 4-225 Millard Hall, University of Minnesota, 435 Delaware St. SE, Minneapolis, MN 55455. Tel: (612) 625-6454. FAX: (612) 625-2163. E-mail: lipsc001@maroon.tc.umn.edu. M.T.S.: Department of Chemistry, 207 Pleasant St. S.E., University of Minnesota, Minneapolis, MN 55455. Tel: (612) 624-1019. FAX: (612) 626-7541. E-mail: stankovi@chemsun.chem.umn.edu.

‡ Department of Biochemistry.

§ Center for Metals in Biocatalysis.

|| Present address: Department of Pharmaceutical Chemistry, University of California−San Francisco, San Francisco, CA 94143.

⊥ Department of Chemistry.

Present address: Diametrics Medical, Inc., 2658 Patton Rd., St. Paul, MN 55113.

⊗ Abstract published in *Advance ACS Abstracts,* April 1, 1997.

[1] Abbreviations: CD, circular dichroism spectroscopy; $E_m°'$, standard midpoint potential; ENDOR, electron nuclear double resonance spectroscopy; EPR, electron paramagnetic resonance spectroscopy; MCD, magnetic circular dichroism spectroscopy; MMO, methane monooxygenase; MMOB, MMO component B; MMOH, MMO hydroxylase component; MMOR, MMO reductase component; MOPS, 3-(*N*-morpholino)propanesulfonic acid; SHE, standard hydrogen electrode; EXAFS, extended X-ray absorption fine structure.

S0006-2960(96)02743-2 CCC: $14.00

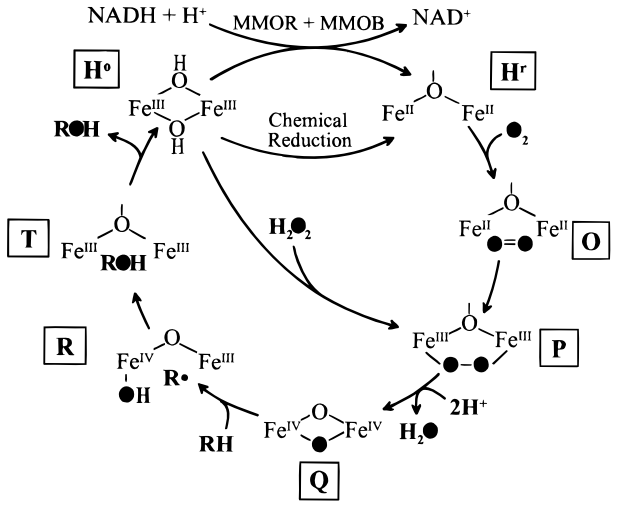

FIGURE 1: Proposed catalytic cycle of MMOH in the presence of substrate and MMOB. All of the intermediates except compound R have been directly observed or are indicated by kinetic studies. [For a summary, see Wallar and Lipscomb (1996).] The solid filled oxygen atoms represent those proposed to be derived from O_2.

oxidation occurs without MMOR.[2] Moreover, the initial velocity of NADH oxidation or product formation is very slow unless MMOB is also present in the reaction mixture. MMOB has been shown to increase the rate of NADH coupled substrate oxidation by as much as 150-fold for some substrates (Fox et al., 1991).

It has long been suspected that MMOB plays some regulatory role in catalysis, perhaps related to the need of all monooxygenase enzymes to limit uncoupled turnover (Fox et al., 1989). In past studies, we and others have shown that MMOB has many such effects on catalysis that derive from formation of a high-affinity complex with MMOH which alters the environment, and consequently the spectroscopic (Fox et al., 1989, 1990a; Froland et al., 1992; Pulver et al., 1993) and chemical properties (Liu & Lippard, 1991, 1995; Froland et al., 1992; Paulsen et al., 1994; Liu, Y., et al., 1995) of the diiron cluster. Potentiometric studies of the enzyme isolated from *M. trichosporium* OB3b have shown that the overall midpoint potential of MMOH decreases from +48 to −84 mV when the complex with MMOB is formed (Paulsen et al., 1994). Accordingly, diferric MMOH was shown to have 4−5 orders of magnitude higher affinity for MMOB than diferrous MMOH. Several intermediates in the MMO catalytic cycle have recently been detected and characterized, as summarized in Figure 1 (Lee et al., 1993a,b; Liu, Y., et al., 1995; Liu, K. E., et al., 1995a,b; Liu & Lippard, 1995; Shu et al., 1997). Recently, we have shown that the overall rate of reaction of diferrous MMOH with O_2 to form a transient reaction cycle intermediate termed compound P is increased 1000-fold upon formation of a complex with MMOB (Liu, Y., et al., 1995). This has the effect of shifting the rate-limiting step in catalysis to intermediates that occur later in the cycle which either react directly with hydrocarbon substrates (compound Q) to yield enzyme-bound products, or release these products (compound T). This oxygen gating effect of MMOB stimulates MMOH such that the overall rate of turnover is maximized and the steady state concentrations of intermediates (e.g., compound P) that might uncouple the reaction are minimized.

Some results have suggested that, in addition to its role as a supplier of electrons, MMOR may also serve regulatory functions that complement those of MMOB. For example, the yield of hydroxylated product from the reconstituted, NADH coupled MMO system which includes MMOR is nearly 100% (Fox et al., 1989), while in single turnover systems that do not contain MMOR lower yields are observed (Liu, Y., et al., 1995). Also, MMOR has been observed to cause a shift in the distribution of products from substrates that can be oxidized in more than one position when added to single-turnover systems (Froland et al., 1992), suggesting that it causes some change in the way MMOH interacts with substrates. Quantitation of MMOR binding to MMOH monitored by changes in endogenous fluorescence showed that MMOR binds at two different sites with affinities that differ by 3 orders of magnitude (Fox et al., 1991). The affinity of only one of these sites fulfills the requirements for the complex in which electrons are transferred based on kinetic studies, suggesting that the second site may play a different role. Finally, in our previous study of the interaction of MMOH and MMOB, we reported preliminary data indicating that MMOR can alter the midpoint redox potential of MMOH, suggesting that it may regulate its own electron transfer in some way (Paulsen et al., 1994).

In this study, the regulatory effects of MMOR on the redox potentials of MMOH and its complexes, the kinetics of various steps within the reaction cycle, and the overall product yield of catalysis are examined. It is shown that MMOR has profound effects on each of these aspects of the function of MMOH as a catalyst. Together, the effects of MMOR and MMOB on MMOH turnover appear to represent a novel mechanism for regulation of catalytic efficiency and rate in an oxygenase system.

EXPERIMENTAL PROCEDURES

Enzyme Purification, Characterization, and Assay. The growth of *M. trichosporium* OB3b, the purification, and the characterization of the soluble methane monooxygenase were as previously reported (Fox et al., 1989, 1990b). Concentrations of protein components were determined by quantitative amino acid analysis for experiments involving redox titrations and by optical absorption for other experiments. The iron content of MMOH was determined by inductively coupled plasma emission spectroscopy (Fox et al., 1989). The specific activities at 23 °C and iron content of the enzyme preparations used for these studies are as follows: MMOH, 600−1000 nmol/(min·mg), 1.8−2.0 diiron clusters/mol; MMOB, 7000 nmol/(min·mg); and MMOR, 11 000 nmol/(min·mg).

Chemicals. The redox mediators used for the electrochemical titrations were the same as previously described (Paulsen et al., 1994). All other chemicals were obtained from Sigma or Aldrich Chemical Co. and were used without further purification. High-purity (99.99%) methane gas was purchased from Air Products Co., Shakopee, MN. Water was deionized and glass distilled.

Potentiometric Titrations of Component Complexes. The EPR-spectroelectrochemical cell and titration method have been previously described (Paulsen et al., 1994). All EPR-

[2] MMOR also has redox potentials [FAD^{ox}/FAD^{red} $E_1^{\circ\prime} = -150$ mV, $E_2^{\circ\prime} = -260$ mV Fe_2S_2, $E^{\circ\prime} = -220$ mV, pH 7.0 (Lund & Dalton, 1985)] between those of NADH ($E^\circ = -320$ mV) and MMOH ($E_m =$ 48 mV), allowing for efficient electron transfer.

spectroelectrochemical experiments were performed using 100 mM MOPS (pH 7.0, 4 °C). MMOH was present at 180−230 μM in a starting volume of 1.9 mL. The concentrations of redox mediators used were approximately 30% of the concentration of diiron clusters present in each experiment. Except where noted, MMOB and MMOR were added in stoichiometric amounts relative to the MMOH diiron cluster concentration in order to nearly saturate the MMOH binding sites [K_d < 100 nM for the catalytically relevant binding of both MMOB and MMOR (Fox et al., 1991)]. Sodium dithionite (Aldrich) was used as the reductant. It was prepared in anaerobic buffered solutions and quantified before use by titration of potassium ferricyanide solution (ϵ_{420} = 1.03 mM^{-1} cm^{-1}). The equilibration time was 1−2 h for each sample. Equilibrium was assumed to be achieved when the system potential was stable for at least 20 min, and then the sample was removed and anaerobically transferred to an EPR tube. All EPR samples were rapidly frozen in cold isopentane (∼−160 °C) and then transferred to liquid nitrogen.

Data fitting and analysis were as previously described (Paulsen et al., 1994). Error was estimated as the cumulative contributions of EPR quantitation (±10 %), diiron cluster concentration from quantitative amino acid analysis and iron determination (±3%), and system potential determination (±2 mV), leading to a maximum fitting error of approximately ±15 mV.

Potentiometric Titrations of MMOH and Its Complexes in the Presence of Methane. Potentiometric titrations of MMOH and component complexes in the presence of methane were performed under similar conditions to those described above. However, after the cell was made anaerobic with argon, the headspace gas of the cell was replaced by methane at a pressure of 5.3 psi. A period of equilibration was allowed with constant stirring of protein solution to ensure that all the active sites of MMOH were saturated with methane. The gas line connected to the methane tank was equipped with a Ridox oxygen scrubber (Fisher Scientific Co., Fair Lawn, NJ) in order to deplete any trace oxygen which may have been in the methane, since the presence of oxygen would allow turnover by diferrous MMOH to generate oxidized MMOH and methanol.

A Henry's law constant (K_i) of 3.7 × 10^5 psi was used to calculate the mole fraction (X_i) of methane gas present in aqueous solution at 4 °C and at a pressure (P_i) of 20 psi (X_i = 5.4 × 10^{-5}). The concentration (C_i) of methane present in aqueous solution (3.0 mM) was then calculated from the equation

$$C_i = (\rho_a X_i)/M_a$$

where ρ_a and M_a are the density (4 °C) and molecular weight of water, respectively. The dissociation constant (K_d) for methane bound to the oxidized, mixed valence, or reduced MMOH has not been measured. However, the K_M value for methane at 4 °C is approximately 12 μM (Nesheim & Lipscomb, 1996); thus it is likely that, at 3.0 mM, all sites will be saturated if the binding of methane to these stable states of MMOH is relevant to turnover.

EPR Spectra Measurements and Data Analysis. Low-temperature X-band EPR spectra were recorded using a Varian E-109 spectrometer and an Oxford Instruments ESR-910 liquid helium cryostat as previously described (Fox et al., 1989). The standard used for spin quantitation was a 1.0 mM $Cu(ClO_4)_2$ solution. Spin quantitations were performed by double integration of spectra measured at non-saturating microwave power levels according to previously described procedures (Aasa & Vänngård, 1975; Fee, 1978; Fox et al., 1991). After the quantitation, the data were plotted as the fraction of mixed valence state versus the measured potential value at each point in the titration. The data were fit using the nonlinear regression program according to the equation derived from the Nernst equation as previously described (Paulsen et al., 1994).

Stopped-Flow Absorption Spectroscopy Experiments. Single-turnover reactions by diferrous MMOH were monitored using a stopped-flow apparatus (Update Instruments, Inc.) as described previously (Lee et al., 1993b). In general, MMOH (60 μM, 120 μM active sites) and methyl viologen (10 μM) were made anaerobic in 100 mM MOPS, pH 7.7. Sodium dithionite was added stoichiometrically (2 reducing equiv/active site) to reduce MMOH. Anaerobic MMOB was added to the reduced MMOH to give a final concentration of 120 μM. The enzyme solution was then loaded anaerobically into one stopped-flow syringe. The other stopped-flow syringe was loaded with O_2-saturated buffer. After the solutions were rapidly mixed at 4 °C, absorbance changes were monitored at 430 nm. When MMOR was used in the reduced state, it was reduced at the same time as MMOH with sodium dithionite (3 equiv/protein) and therefore was present in the same stopped-flow syringe as MMOH and MMOB. When oxidized MMOR was used, it was added to the O_2-containing syringe. For all experiments, O_2 was added in large excess over MMOH. Complete reduction of MMOH was indicated by the residual weak blue color from a fraction of the methyl viologen in the one-electron reduced state. Oxygen was shown to react at least 3 orders of magnitude more rapidly with methyl viologen than with the reduced MMOH so that no excess reducing equivalents entered the reaction from this source.

Kinetic Data Analysis. The reaction kinetics could be analyzed as one or more exponential phases using the nonlinear regression program KFIT developed by Dr. N. C. Millar, Kings College, London, as previously described (Lee et al., 1993b). Simulations of reaction time courses based on mechanistic proposals were performed using the numerical integration program KSIM, also developed by Dr. Millar (Liu, Y., et al., 1995).

Freeze Quench Techniques and EPR Analysis. The experiments were carried out as described above for stopped-flow experiments except that MMOH was in higher concentration (200−300 μM, MMOB at 400−600 μM). The procedures for the freeze quench techniques were as described previously (Lee et al., 1993b). EPR spectra were recorded and analyzed as described above.

Product Yield Determinations for Single-Turnover Reactions. Diferrous MMOH (300 μM with or without MMOB) solutions were prepared as described above. Propene gas (99%) was bubbled through a sodium dithionite solution to remove any O_2 impurity and then added to the headspace of the protein sample vessel at 1 atm and allowed to equilibrate to make a saturated solution, estimated to be 7.3 mM (Fogg & Gerrard, 1991). Single-turnover reactions were initiated by the addition of 150 μL of the protein solution to an equal volume of 100% O_2-saturated buffer in a vial containing 100% O_2 in the headspace, at 4 °C. For experiments in

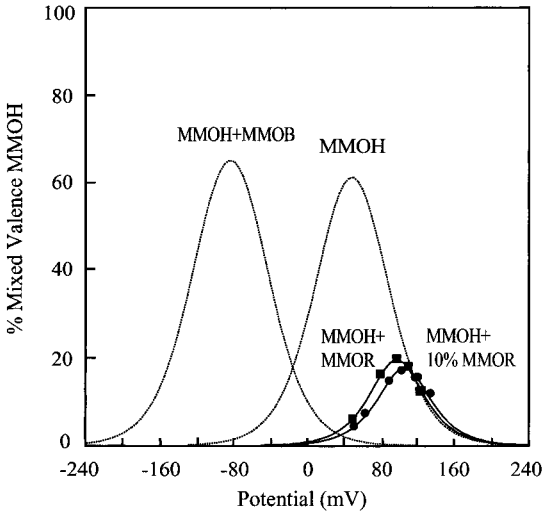

FIGURE 2: Fraction of mixed valence state of MMOH stabilized during the reductive titration of the MMOH−MMOR complex at different system potentials. MMOR is present at ratios of 0.1 (●) and 1.0 (■) relative to MMOH active site concentration. See the Experimental Procedures for conditions of the experiment. The experimentally determined titration curves for MMOH and the MMOH−MMOB complex are shown for comparison (Paulsen et al., 1994). The relevant parameters are listed in Table 1.

which reduced MMOR was present, it was added to the MMOH solution prior to addition of sodium dithionite. When oxidized MMOR was used, it was added to the O_2-saturated buffer. Any small excess of sodium dithionite reacts much more rapidly O_2 than with oxidized MMOR or diferric MMOH produced by turnover. After the reaction had been allowed to go to completion (10 min), duplicate 100 μL aliquots of the reaction mixture were removed and the reactions were quenched by addition of an equal volume of $CHCl_3$. The solution was mixed with a vortex and centrifuged, and the product, propene oxide, in the $CHCl_3$ layer was analyzed by gas chromatography as previously described (Liu, Y., et al., 1995).

Peroxide Shunt Reaction. Diferric MMOH (50 μM) was incubated with or without MMOB and/or MMOR in the presence of 20 mM H_2O_2 and 7.3 mM propene. The reaction conditions were 4 °C, 100 mM MOPS, pH 7.7. Samples were withdrawn at 2, 5, 10, and 20 min during the course of each reaction, and the reaction was stopped by addition of an equal volume of $CHCl_3$. The concentration of propene oxide produced was determined by gas chromatography as described above. Each reaction gave a linear rate of propene oxide production over the 20 min reaction from which the rate was calculated.

RESULTS

Formal Redox Potential Values of MMOH−MMOR Complex. The results of a redox titration of a 1:1 MMOR:MMOH (sites) complex are shown in Figure 2 (■), and the formal redox potentials are summarized in Table 1. In this titration, the EPR spectrum of the mixed valence state of MMOH in the complex was quantitated by double integration. In a previous study, we showed that there is no spectroscopic evidence for binding of the redox mediator dyes present in the titration solution to MMOH and that double integration of the EPR spectrum gives an accurate quantitation of the mixed valence state (Paulsen et al., 1994). The formal redox potential values for the first and second electron transfers are $E_1^{\circ\prime} = +80 \pm 15$ mV and $E_2^{\circ\prime} = +114 \pm 15$ mV, respectively, at 4 °C, pH 7.0. Thus, the overall midpoint potential value (+97 mV) is 49 mV more positive for the MMOH−MMOR complex than for MMOH alone. Interestingly, the maximum percentage of the mixed valence state that could be thermodynamically stabilized is only 19%, which is much less than the 61% observed for uncomplexed MMOH (Paulsen et al., 1994). This is consistent with the observation that the relative magnitudes of $E_1^{\circ\prime}$ and $E_2^{\circ\prime}$ are reversed for MMOH−MMOR compared with MMOH such that the second electron transfer is more favorable than the first. In accord with the measured redox potentials, the amount of diferrous MMOH (monitored by the characteristic EPR signal near $g = 16$ for this state) is greater for the MMOH−MMOR complex than for MMOH alone at any fixed system potential [data not shown, but see Paulsen et al. (1994)].

The effect of the ratio of MMOR to MMOH on the redox potential values of MMOH was also investigated. Surprisingly, it was found that the addition of MMOR at only 10% of the amount of MMOH active sites caused the redox potential values of MMOH to completely shift to the same values as observed for MMOH complexed with a stoichiometric amount of MMOR. As shown in Figure 2 (●), the formal redox potential values for the first and second electron transfers of the 0.1:1 MMOR:MMOH complex were $E_1^{\circ\prime} = +85 \pm 15$ mV and $E_2^{\circ\prime} = +125 \pm 15$ mV, respectively (overall midpoint potential $E_m = +105$ mV, maximum mixed valence state = 18%). As a control, the effect of mercaptoacetic acid, the stabilizing reagent present in the MMOR preparation, on MMOH−MMOB midpoint potential was examined. At a fixed system potential of approximately −15 mV, no change in the relative amounts of mixed valence and diferrous MMOH was observed upon addition of mercaptoacetic acid, indicating that it does not affect the midpoint potentials (data not shown).

Formal Redox Potential Values of MMOR−MMOB−MMOH Complex. Figure 3 (■) shows the potentiometric data obtained from the EPR−spectroelectrochemical titration for the 1:1:1 MMOR:MMOB:MMOH (sites) ternary complex. Previous results of steady state kinetics and component binding studies (Fox et al., 1991) suggest that 1 MMOB and 1 MMOR per MMOH active site is enough to nearly saturate all the dinuclear iron clusters of MMOH at the concentrations used for the redox titrations. The formal potential values determined in this work for the ternary complex were $E_1^{\circ\prime} = +76 \pm 15$ mV and $E_2^{\circ\prime} = +125 \pm 15$ mV for the first and second electron transfers, respectively (overall midpoint potential $E_m = +100$ mV, maximum mixed valence state = 15%). These values are the same as the redox potential values of MMOH−MMOR complex indicated above within experimental error. Thus, MMOR binding caused the midpoint potential value of MMOH−MMOB complex (−84 mV) to shift 184 mV positively and the $E_1^{\circ\prime}$ and $E_2^{\circ\prime}$ values to be reversed as observed for the MMOH−MMOR complex. These results suggest that MMOR binding is the dominant factor in establishing the MMOH redox potential in the reconstituted system and that it thermodynamically stabilizes the catalytically active diferrous MMOH species. MMOR does not cause this effect by forcing the dissociation of MMOB because the line shape of the mixed valence EPR signal observed throughout the potentiometric titration is

Table 1: Summary of the Redox Potential Values of MMOH and its Complexes with MMOB, MMOR and Methane

MMO component or complex[c]	*M. trichosporium* OB3b[a] $E_1°'$ (mV)[d]	$E_2°'$ (mV)[d]	E_m (mV)[d]	maximum mixed-valence (%)	*M. capsulatus* (Bath)[b] $E_1°'$ (mV)[d]	$E_2°'$ (mV)[d]	E_m (mV)[d]
MMOH	76	21	48	61	100	−100	0
MMOH−MMOB (1:2)	−52	−115	−84	65	50	−170	−60
MMOH−MMOR (1:1)	80	114	97	19			
MMOH−MMOR (1:0.1)	85	125	105	18			
MMOH−MMOB−MMOR (1:1:1)	76	125	100	15	< −200	< −200	
MMOH−MMOB−MMOR (1:2:0.1)	109	75	92	50			
MMOH + CH_4	72	−33	20	82	30[d]	−156	−63
MMOH−MMOB (1:1) + CH_4	−48	−119	−84	69			
MMOH−MMOB−MMOR (1:1:1) + CH_4[e]	70	128	99	13	< 100[d]	100	

[a] Values for *M. trichosporium* OB3b MMOH and MMOH−MMOB from Paulsen et al. (1994). [b] Values for *M. capsulatus* (Bath) MMO from Liu and Lippard (1991, 1995). [c] The stated ratios of components refer to those used in the experiments utilizing the *M. trichosporium* OB3b MMO (sites). [d] Represents the formal redox potential values for the first electron transfer ($E_1°'$), second electron transfer ($E_2°'$), and the overall midpoint potential value $E_m = (E_1°' + E_2°')/2$. Values given are relative to SHE. Error = ±15 mV. [e] Substrate was propene for the *M. capsulatus* (Bath) MMO studies. Propene has essentially no effect on the *M. trichosporium* OB3b MMOH potentials (Paulsen et al., 1994).

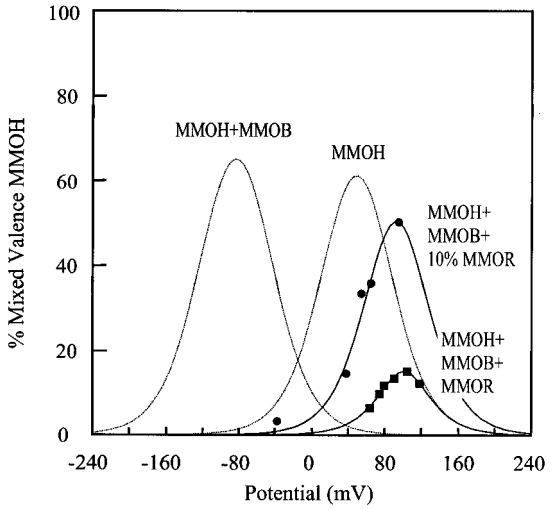

FIGURE 3: Fraction of mixed valence state of MMOH stabilized during the reductive titration of the MMOH−MMOB−MMOR complex at different system potentials. MMOR is present at ratios of 0.1 (●) and 1.0 (■) relative to MMOH active site concentration. See the Experimental Procedures for conditions of the experiment. The experimentally determined titration curves for MMOH and the MMOH−MMOB complex are shown for comparison (Paulsen et al., 1994). The relevant parameters are listed in Table 1.

characteristic of the MMOH−MMOB complex (Fox et al., 1991) (data not shown).

The addition of a substoichiometric amount of MMOR to the MMOH−MMOB complex [MMOH:MMOB:MMOR (sites) = 1:2:0.1] also causes the redox potential values of MMOH to undergo a positive shift as observed for the stoichiometric complex. As shown in Figure 3 (●), the formal redox potential values for this complex were $E_1°'$ = +109 ± 15 mV and $E_2°'$ = +75 ± 15 mV, respectively (overall midpoint potential E_m = +92 mV, maximum mixed valence state = 50%). The overall midpoint potential value of this complex is similar to that of the MMOR−MMOB−MMOH complex except the $E_1°'$ and $E_2°'$ values are not reversed ($E_1°' > E_2°'$). This incomplete shift may be due to the presence of a mixture of species. We have observed the formation of an MMOB−MMOR complex in solution and measured its binding constant (Fox et al., 1991). When MMOB is in large excess, this complex will reduce the amount of free MMOR and decrease MMOH−MMOR complex ratio significantly below 1:0.1. We have also shown that excess MMOB disrupts the MMOH−MMOR complex. Thus, more MMOR may be required to observe the complete shift in potentials when MMOB is present in excess.

Formal Redox Potential Values of MMOH and Its Component Complexes in the Presence of Methane. The addition of a saturating concentration of methane to MMOH alone or to its complexes with MMOR and MMOB caused little change in the formal redox potentials determined from EPR-spectroelectrochemical titrations; the data are presented in Table 1. Thus, the binding of the natural substrate methane is not a significant factor in the regulation of the redox potentials of the *M. trichosporium* MMO enzyme system.

Effect of MMOR on the Reaction of Diferrous MMOH with O_2. MMOH must be in the diferrous redox state to undergo any reaction with O_2 (Fox et al., 1989). The kinetics of this reaction are conveniently monitored using freeze quench transient kinetic techniques in which EPR spectroscopy is used to follow the rate of disappearance of the signal at g =16 characteristic of the integer spin diferrous state (Lee et al., 1993b). We have shown previously that MMOB accelerates the reaction between diferrous MMOH and O_2 to form compound P approximately 1000-fold (Liu, Y., et al., 1995). In contrast, as shown in Figure 4, oxidized MMOR has virtually no effect on the relatively slow reaction of diferrous MMOH with O_2 in the absence of MMOB (0.023 versus 0.031 s^{-1}). However, addition of oxidized MMOR to the MMOH−MMOB complex decreases the rate of the reaction from 22 to 1.25 ± 0.3 s^{-1}. This decrease is not sufficient to make the reaction with O_2 rate limiting for any organic substrate, but it does indicate that there is a complex interaction between all three components that affects O_2 reactivity. Surprisingly, the ~20-fold decrease in the reaction rate with O_2 is also observed for the 1:1:0.1 MMOH:MMOB:MMOR (sites) complex (Figure 4). Thus, substoichiometric MMOR affects this reaction in a similar manner to its affect on the redox potentials of the MMOH−MMOB complex described above.

Effect of MMOR on the Formation and Decay Rates of Compound Q. We have previously shown that the formation and decay rate constants of compound Q depend critically on the degree of saturation of the MMOH−MMOB complex, since the rates of conversion of diferrous MMOH to compound P and compound P to compound Q are both greatly accelerated in the complex (Liu, Y., et al., 1995). Accordingly, the observed decrease in the rate of reaction

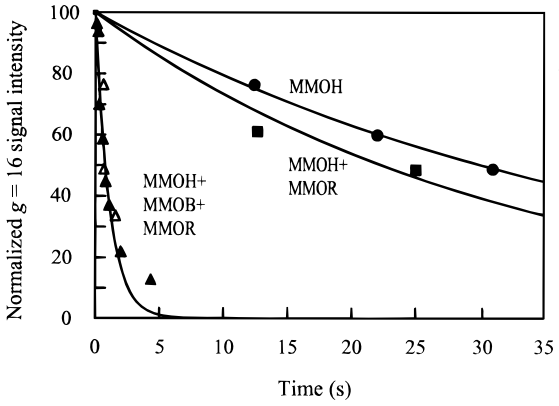

FIGURE 4: Effect of MMOR on the time course of the decay of the $g = 16$ EPR signal from diferrous MMOH after addition of O_2 at 4 °C. Freeze quench samples were prepared as described in Experimental Procedures. MMOR was present in the reactions of the diferrous MMOH−MMOB−MMOR complex at either stoichiometric (▲) or 0.1 equiv (△) relative to MMOH sites. Both data sets are fit with the same rate constant of 1.25 s^{-1}. The rate constant for the reaction of diferrous MMOH−MMOB with O_2 has previously been shown to be 22 s^{-1}. Reactions of diferrous MMOH alone (●) and MMOH−MMOR (■) were fit with rate constants of 0.023 and 0.031 s^{-1}, respectively. For these reactions, additional data points at longer times were collected and used in the fitting procedure but are omitted from the plot shown for clarity.

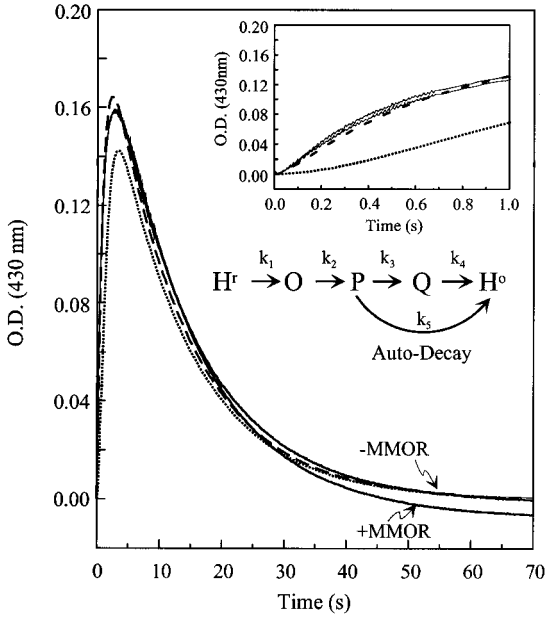

FIGURE 5: Effect of MMOR on the time course for the formation and decay of compound Q. Diferrous MMOH:MMOB (1:2) or diferrous MMOH:MMOB:MMOR (1:2:0.1) was mixed with O_2-saturated buffer using a stopped-flow device as described in Experimental Procedures. The experimental data are shown in solid lines, and the simulations based on the reaction scheme shown on the figure are in broken lines. The two sets of experimental data nearly superimpose in all sections of the time course. Inset: Time course for the reactions at short times after mixing. The rate constants used for the simulations of MMOH−MMOB−MMOR (- - -) were $k_{1-5} = 500$, 1.25, 20, 0.08, and 2.2, s^{-1}, respectively. For comparative purposes, a simulation is shown for the MMOH−MMOB−MMOR reaction (•••), $k_{1-5} = 500$, 1.25, 1.3, 0.07, and 0.3 s^{-1}, respectively, in which only the rate constant for the O to P reaction is changed from the set of values previously determined for the MMOH−MMOB reaction (Liu, Y. et al., 1995). This results in a significant lag phase early in the reaction (see inset) which is not observed experimentally. H^r = diferrous MMOH; H^o = diferric MMOH; O, P, and Q represent the reaction cycle intermediates described in Figure 1.

of the MMOH−MMOB complex with O_2 in the presence of MMOR should lead to dramatic and predictable changes in the time course of formation of compound Q. As shown in Figure 5, subtle changes are observed; however, much larger changes would be expected if the only change were the decrease in the rate of the diferrous MMOH−MMOB conversion to compound P. This is especially true for the shape of the compound Q formation time course curve in the first second of the reaction where a distinct lag phase was expected but not observed (Figure 5, inset). One possibility to account for this observation is that the rate of another step in the sequence leading to compound Q is increased in rate to compensate for the slow formation of compound P. A reasonable candidate for this is the conversion of compound P to compound Q because the rate of this step is apparently affected by complexation of the other regulatory component, MMOB. If the rate of reaction of diferrous MMOH−MMOB in the presence of MMOR is fixed at 1.25 s^{-1}, then a good fit for (i) the shape of the kinetic curve during the first second, (ii) the observed time when compound Q maximizes (t_{max}), and (iii) the maximum amplitude for compound Q (A_{max}) is obtained when the rate of compound P to compound Q is increased to approximately 20 s^{-1} (Figure 5 and inset). A direct observation of the time course of compound P will be required to further evaluate this possibility; this is experimentally difficult due to the facts that compound P is essentially colorless and diamagnetic.

Effect of MMOR on MMOH Single-Turnover Product Yield. The oxidation of propene during a single turnover of diferrous MMOH and MMOH−MMOB (1:2) proceeds with yields of 40% and 80%, respectively (Liu, Y., et al., 1995). As shown in Table 2, addition of oxidized MMOR enhances the product yield by ∼10% when present at 0.1, 0.5, and 1 equiv relative to MMOH, in both the absence and the presence of MMOB. The maximum yield when oxidized MMOR and MMOB are both present is ∼90% assuming that the dinuclear iron sites of MMOH are fully populated; quantitation of the centers reproducibly indicates between 90% and 100% population. In the presence of MMOB, addition of reduced MMOR at 0.1 and 0.5 MMOH equiv increases the respective product yields by 18% and 42%, probably by transferring stored electrons to oxidized MMOH and initiating a second turnover of a subpopulation of MMOH, in combination with the effects of oxidized MMOR. In the absence of MMOB, reduced MMOR decreases the yield of a single turnover. It is not clear why this occurs, but it may involve direct reduction of a highly oxidized intermediate such as compound Q before it can react with substrate. This is potentially a very significant general problem for catalysis by enzymes that generate high-valent reactive species, and our results may indicate yet another role for MMOB in protecting this species in the MMOH cycle from adventitious reduction. In the absence of MMOB, when reduced MMOR is added at 0.1 equiv, the yield is lower than observed for 0.1 equiv of oxidized MMOR but still higher than in the absence of MMOR, possibly indicating a competition between yield increasing and decreasing processes. This is supported by the observation that addition of stoichiometric reduced MMOR significantly decreases the product yield.

These results are in accord with our previous proposal that the loss of yield in the product correlates with a buildup of compound P, which may autodecay without producing

Table 2: Effect of MMOB and MMOR on the Product Yield of a Single Turnover of Diferrous MMOH in the Presence of Propene[a]

reaction[b] additions to $MMOH^r$	product yield[c,d] (%)	yield relative[d] to $MMOH^r$ + 2 MMOB + O_2
+ O_2	40	0.5
+ 0.1 MMOR°, O_2	44	0.55
+ 1 MMOR°, O_2	43	0.54
0.1 $MMOR^r$ + O_2	41	0.51
1 $MMOR^r$ + O_2	12	0.15
2 MMOB + O_2	80	1
2 MMOB + 0.1 MMOR°, O_2	89	1.11
2 MMOB + 0.5 MMOR°, O_2	88	1.10
2 MMOB, 0.1 $MMOR^r$ + O_2	94	1.18
2 MMOB, 0.5 $MMOR^r$ + O_2	114	1.42

[a] Reactions were performed and products analyzed as outlined in Experimental Procedures. [b] Values preceding the component refer to the concentration relative to MMOH. Species separated by commas were added together before mixing with the other species listed after the "+" sign. $MMOH^r$ = diferrous MMOH; $MMOR^r$ = fully reduced MMOR. [c] Based on the total dinuclear iron clusters present, assuming full population of the MMOH active sites. [d] The error in the absolute yield of product is ±10% due to enzyme preparation variability. In contrast, the error in the yield relative to HB is ±4% because the yields from all component combinations change in concert for a given enzyme preparation. Each reaction was repeated six times.

Table 3: Effects of Component Complex Formation on the H_2O_2 Coupled Diferric MMOH Oxidation of Propene[a]

enzyme component(s)	rate[b] relative to MMOH alone (%)
MMOH	100
MMOH, MMOR (1:1)	100
MMOH, MMOR (1:0.1)	68
MMOH, MMOB (1:2)	69
MMOH, MMOB, MMOR (1:2:0.1)	86
MMOH, MMOB, MMOR (1:2:1)	101
MMOH, MMOB, MMOR (1:2:2)	107

[a] Reactions were performed and products analyzed as outlined in Experimental Procedures. Reactions conditions were 4 °C, 100 mM MOPS, pH 7.7. H_2O_2 and propene were initially present at 20 and 7.3 mM, respectively. [b] Error ±10%. Each reaction was repeated in triplicate.

hydroxylated product. MMOR decreases the rate of formation of compound P and probably increases its rate of conversion to compound Q (see Figure 5 for data and simulation). As a result, less of this intermediate will accumulate, thereby limiting what is apparently the major uncoupling reaction of the catalytic cycle.

Effect of MMOR on the Rate of the MMOH Peroxide Shunt. In previous work we have shown that diferric MMOH is capable of catalyzing oxidation of the entire range of MMO substrates in the absence of MMOR and MMOB if it is provided with H_2O_2 (Andersson et al., 1991). This peroxide shunt is inhibited by MMOB for most substrates (Froland et al., 1992). Table 3 shows that this inhibition is overcome by a stoichiometric concentration of MMOR.

DISCUSSION

This study has demonstrated further regulatory roles of MMOB and has revealed two new aspects of the interaction of MMOH and MMOR. First, it is clear that MMOR is able to optimize its primary role as an electron transfer partner for MMOH by coupling binding and redox potential energy to establish a larger driving force while adjusting the individual midpoint potentials for the diiron cluster so that the catalytically active two-electron reduced form is favored. Second, MMOR appears to play a more subtle role by favorably modulating the rates of interconversion of the catalytic cycle intermediates so that the product yield from the system becomes tightly coupled to the energy available for the reaction. Both the mechanism(s) by which MMOR accomplishes these two roles and the manner in which MMOR and MMOB interact with MMOH to influence catalysis are quite unusual. The significance to the mechanism of MMO and the relevance to enzyme regulation in general are discussed in the following sections.

Comparison with the Redox Potential Studies of MMO from M. capsulatus (Bath). As shown in Table 1, the redox potential values for *M. trichosporium* OB3b MMO are significantly different than the values reported for *M. capsulatus* (Bath) MMOH and its component complexes (Liu & Lippard, 1991, 1995). For the latter enzyme, addition of an unresolved mixture of MMOB and MMOR caused the formal redox potential values of MMOH to shift to the negative by at least 300 mV so that it could not be reduced under the conditions of the experiment (system potential, −200 mV). The opposite phenomenon is reported here for *M. trichosporium* MMOH, in that addition of MMOB and MMOR caused MMOH to be more easily reduced by increasing the midpoint potential substantially. Another difference is that addition of a substrate to the MMOH−MMOB−MMOR complex in the *M. capsulatus* system caused an increase in potential of more than 400 mV, whereas in the current studies, we find no substantial effects of the substrate methane on the potential of MMOH or its component complexes. Our result is in accord with several different types of observations which indicate that substrate does not add to the enzyme in early stages of its catalytic cycle in any mechanistically relevant fashion. These include (i) no major changes are observed in UV−vis, Mössbauer, EXAFS, EPR, CD, MCD, and ENDOR spectra of the oxidized, mixed valence, and diferrous forms of the enzyme are observed when substrates such as methane are added (Hendrich et al., 1992; Pulver et al., 1993; DeWitt et al., 1995); (ii) transient kinetic studies have shown that methane has no effect on the formation or decay rate of any intermediate in the catalytic cycle prior compound Q. In the case of compound Q, the formation rate is similarly unaffected, but methane causes the decay rate to increase linearly with the concentration added (Lee et al., 1993b; Nesheim & Lipscomb, 1996). This shows that substrate does not participate in any step in which these intermediates are formed or any step reversibly connected to these steps. The linear relationship between the compound Q decay rate and the added substrate concentration suggests that the substrate reacts directly with compound Q resulting in its decay. The first intermediate observed after the decay of compound Q is compound T which is a product complex of the enzyme. Thus, it is likely that the first interaction of substrate with MMOH that is significant to catalysis is with compound Q, not with diferric or diferrous MMOH. These results indicate the regulation of catalysis for MMO OB3b is more likely to involve component−component than substrate−component interactions. Specifically, a regulatory mechanism in which substrate binding modulates electron transfer from NADH into the hydroxylase, as proposed for cytochrome $P450_{cam}$ (Sligar & Gunsalus, 1976) and MMOH Bath (Liu & Lippard, 1991), is unlikely for MMOH OB3b.

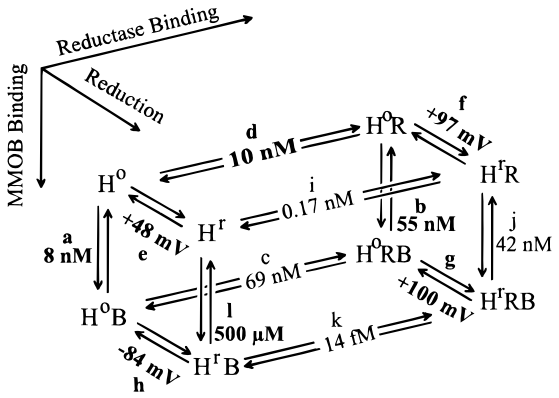

FIGURE 6: Thermodynamic state diagram summarizing the energetics of coupling of MMOH reduction, MMOB binding, and MMOR binding. The values indicate dissociation constants for component complexes and standard reduction midpoint potentials for the redox processes. This mechanism would pertain if a true equilibrium is reached and there is only one type of interaction between MMOR and MMOH. The values shown in bold type were determined experimentally, while the others were calculated assuming standard equilibrium thermodynamics as outlined in the text. Compiled from Fox et al. (1991), Paulsen et al. (1994), and the current study. H^r = diferrous MMOH; H^o = diferric MMOH; R = MMOR; B = MMOB.

Recent crystallographic studies corroborate multiple spectroscopic studies, showing that the structures of MMOH OB3b (Elango et al., 1997) and MMOH Bath (Rosenzweig et al., 1993, 1995) are remarkably similar. This similarity does not appear to support the large differences in the effects of component and substrate complexes on redox potential that have been described.

Thermodynamic Relationships between Component Association and Reduction. In previous work, we have shown that the 132 mV decrease in the E_m of MMOH associated with MMOB binding indicates approximately a 4−5 orders of magnitude decrease in the affinity between these components upon reduction of the MMOH (Paulsen et al., 1994). In contrast, we show here that complexation of MMOR causes the E_m of MMOH to shift to the positive by about 49 mV, implying an increase in affinity at equilibrium. There are several ways to place this observation in the context of regulation in the system. The most straightforward way is to assume that the effects of MMOR derive from a stoichiometric complex with MMOH which reaches a true equilibrium. In this case, the 49 mV increase in the E_m of MMOH associated with MMOR binding predicts a ~60-fold increase in the affinity between these components upon reduction of the MMOH. Fits to steady state kinetic data and measurement of the dissociation constant of the diferric MMOH−MMOR complex give an approximate K_d of 10 nM (Fox et al., 1991). Thus, at equilibrium, the dissociation constant between the diferrous MMOH and MMOR complex will be about 0.17 nM.

The thermodynamic relationships between the MMOH−MMOB binding, MMOH−MMOR binding, and MMOH reduction can be succinctly summarized by constructing a thermodynamic cube as shown in Figure 6. In this model, only the oxidized and $2e^-$ reduced states of MMOH are considered. Since the free energy to move from any corner of the cube to another must be independent of path, the states within the square unit on each face of the cube can all be related thermodynamically. The values shown in bold for the pathways marked **a**, **b**, **d**, **e**, **f**, **g**, **h**, and **l** have all been determined experimentally, and the values in the rest of the pathways are calculated based on the required path independence. On the top face of the cube, the pathways (**e**, **d**, **f**, i) of the binding with MMOR and the reduction of MMOH are energy coupled. On the left face of the cube, the pathways (**a**, **e**, **h**, **l**) of the binding with MMOB and the reduction of MMOH are energy coupled. The thermodynamic relationships of the species on the corners of these two faces of the cube have already been discussed [preceding discussion and Paulsen et al. (1994)].

The most mechanistically relevant faces of the cube are those which describe the thermodynamic relationships of the redox and binding energies when the MMOH−MMOB or MMOH−MMOR binary complexes bind the third component. For the back face of the cube, steady state kinetics and fluorescence binding studies suggest that diferric MMOH has a strong affinity for MMOB and MMOR, respectively (pathways **a** and **d**). The binding constants of the MMOH−MMOR complex for MMOB and the MMOH−MMOB complex for MMOR (pathways **b** and c) cannot be directly determined using fluorescence spectroscopy. However, steady state kinetics indicated that these dissociation constants were also in the nanomolar range (Fox et al., 1991). Thus, for the right face of the cube, the binding constant between the reduced MMOH−MMOR complex and the MMOB component (pathway j) can be evaluated using the known values of pathways **b**, **f**, and **g**. It appears that the binding of MMOB to the reduced MMOH−MMOR complex is as tight (K_d = 42 nM) as the binding of MMOB to the oxidized MMOH−MMOR complex (pathways j and **b**, respectively) since the redox potential value of the MMOH−MMOR complex is not changed upon MMOB binding (pathways **f** and **g**). Thus, MMOR binding appears to be able to interfere with the coupling between the MMOB binding energy and the redox potentials of MMOH (compare the left and right faces of the cube, Figure 6). That is, the presence of MMOR changes the redox potential values of the MMOH−MMOB complex (pathways **h** and **g**) as well as the binding affinity between the reduced MMOH and MMOB component (pathways **l** and j). On the bottom face of the cube, it seems that the MMOH−MMOB complex has a stronger affinity for MMOR when MMOH is reduced (pathways c and k). This is so because a dramatic redox potential change of MMOH−MMOB complex (pathways **h** and **g**) caused by MMOR binding as well as an affinity change between the reduced MMOH and MMOB upon MMOR binding (pathways **l** and j) were observed. The 184 mV increase in the E_m of MMOH−MMOB complex caused by MMOR binding predicts an increase in the binding affinity between the MMOR and the MMOH−MMOB complex of approximately 6 orders of magnitude (K_d ~ 14 fM when MMOH is reduced). Thus, in this model, MMOB binding will alter the binding affinity between the reduced MMOH and MMOR (compare pathways i and k). This predicted high affinity for MMOR after the MMOH is reduced would have a beneficial effect on catalysis since the presence of MMOR appears to couple NADH consumption to enhanced product formation as indicated in Table 2.

There are many unknowns which are not accounted for by the model in Figure 6. For example, the K_d for the MMOH−MMOR complex determined by fitting steady state data and supported by calculation (pathways **b** and c) may reflect the affinity of MMOR in the reduced state, whereas

oxidized MMOR was present in the direct redox and binding measurements. To properly account for these possibilities would require more dimensions in the thermodynamic state diagram and additional data which is not yet available. In any event, if equilibrium is achieved, it appears that the binding of the third component to any binary complex does change the thermodynamic aspects of the interaction of the first two components.

Alternative Schemes for the Participation of Component Complexes in Regulation. Another way to interpret the data presented here is to abandon the assumption that all of the processes of MMOR and MMOB binding to MMOH and their effects on redox potential that we have measured are directly thermodynamically coupled. The reason to consider an alternative is that the relative concentration of MMOR versus MMOH ± MMOB required to cause changes in the redox potential values is much lower than stoichiometric (see Table 1). This remarkable effect can be accounted for by several mechanisms: (i) Intermolecular electron transfer between MMOH molecules may be very slow in the absence of MMOR, and MMOR may preferentially transfer two electrons to MMOH before dissociating due to the interchange in magnitudes of the redox couples of the diiron cluster when MMOR is present. In this way, the diferrous MMOH would be maintained at an artificially high level by the establishment of a pseudo equilibrium during a redox titration. (ii) The MMOR may provide multiple binding sites for the MMOH, thus allowing a single MMOR molecule to perturb several MMOH molecules simultaneously. (iii) An initial weak MMOH−MMOR complex may form which causes MMOH to convert to a new conformation with different physical properties (MMOH′) which relaxes back to the original conformation very slowly after dissociation of MMOR. If the MMOR dissociation rate is fast relative to the rate of this hysteretic effect, a small amount of MMOR would alter the entire population of MMOH.

Although there is no direct evidence for any of these alternative mechanisms, they can be evaluated to some extent using the data reported here. We have shown that the inhibitory effect of MMOR on the O_2 reactivity of the diferrous MMOH−MMOB complex is fully established when the MMOH:MMOR (sites) ratio is only 1:0.1. This is a single-turnover event involving only diferrous MMOH−MMOB, and thus, a pseudo equilibrium of the type proposed in mechanism (i) would not apply. Oxygen would simply react rapidly with the 90% of the MMOH−MMOB complexes that were not bound to MMOR. Likewise, MMOR increases the single-turnover product yield by ∼10% at both stoichiometric and substoichiometric concentrations, thus a small amount of MMOR affects the stability of the entire population of at least one of the MMOH reaction cycle intermediates in a single-turnover reaction. If the same phenomenon is responsible for the high measured redox potential when MMOR is present, the decreased reactivity of diferrous MMOH−MMOB with O_2, and increased product yield, then mechanism i would not seem to account for all of the results. Mechanism ii cannot be eliminated, but given the size of MMOH relative to MMOR (245 000 versus 38 000) it is difficult to postulate a structural assembly that would permit the required 10 MMOH:1 MMOR (sites) stoichiometry.

Mechanism iii, as illustrated in Figure 7, would meet the requirements of the redox measurements, single-turnover

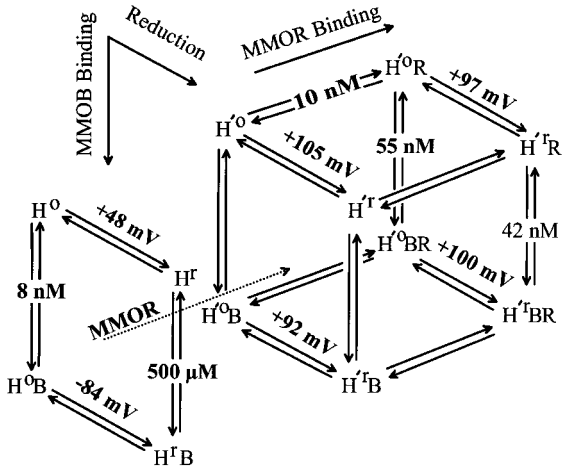

FIGURE 7: Alternate mechanism by which MMOR may exert its regulatory effects. The values indicate dissociation constants for component complexes and standard reduction midpoint potentials for the redox processes. This mechanism would account for the observed effects of MMOR at substoichiometric concentrations. The experimentally determined values are shown in bold, and the calculated values are shown in normal font. H^r = diferrous MMOH; H^o = diferric MMOH; H′ = an altered form of MMOH caused by interaction with MMOR; R = MMOR; B = MMOB. The redox potentials associated with the H′ and H′B face of the cube were obtained by the electrochemical titration under reaction conditions of MMOH:MMOR = 1:0.1. This is taken to be an approximation of the correct values because the extent of formation of the stoichiometric MMOH−MMOR complex would only be about 10% under these conditions.

yield experiments, and the transient kinetic measurements of O_2 reactivity. Under this model, all of the thermodynamic measurements that we have made in which MMOR was present have actually been made with MMOH′ rather than MMOH and thus many of the values associated with the thermodynamic cube of Figure 6 would not apply. In effect, MMOR acts as a catalyst in this model to change the structure of MMOH to that of MMOH′. Therefore, the two thermodynamic cycles describing the interactions of MMOB with MMOH and MMOH′, respectively, become effectively independent. When MMOR is present, the MMOH′ cycle applies, while in its absence, the MMOH cycle pertains (see Figure 7).

Two potential difficulties with this model are the need to assume hysteresis in the MMOH structure and the need to propose that MMOR can dissociate rapidly compared with this hysteretic change. There is ample precedent for hysteretic behavior in the structure of MMOH in our studies of its interactions with MMOB (Fox et al., 1991; Froland et al., 1992). However, the measured dissociation constant of 10 nM for the diferric MMOH′−MMOR complex suggests a long half-life for dissociation (seconds) for typical values of the second-order association rate constant (10^5−10^6 s^{-1} M^{-1}). It should be pointed out, however, that during our direct determination of the MMOH−MMOR K_d value, a second binding site for MMOR was detected with a 1000-fold weaker affinity and equal maximum occupancy as the high-affinity site (Fox et al., 1991). If this site were to be responsible for the conversion of MMOH to MMOH′, then the much weaker affinity would probably allow significantly faster dissociation of MMOR. MMOR would still be trapped by the high-affinity site, which presumably is related to its electron transfer role. Thus, the regulatory function of MMOR would have to be carried out by the very small

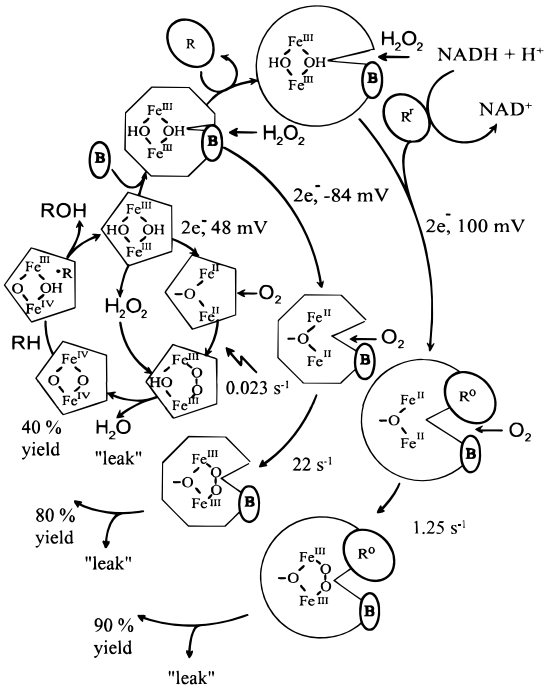

FIGURE 8: Hypothetical scheme by which MMO component complexes may regulate the catalytic cycle of MMOH. R = MMOR; B = MMOB.

amounts present as free MMOR in equilibrium with the component bound in the high-affinity MMOH′ sites.

During normal *in vivo* catalysis, MMOR is thought to be present at 10% of the MMOH concentration[3] so the thermodynamic cycle involving MMOH′ would represent the normal manner in which electron transport and catalytic rate and efficiency are regulated. Accordingly, the redox potential of MMOH′ would remain high and there would be an increased tendency for MMOH′ to accept $2e^-$.

Hypothesis for the Regulatory Roles of MMOB and MMOR during the Catalytic Cycle. In general terms, the roles of MMOB that we have recognized from previous studies are to make the active site of diferrous MMOH more accessible to O_2 and to reduce the redox potential of the diiron cluster in the absence of MMOR (Paulsen et al., 1994; Liu, Y., et al., 1995). The special roles of MMOR recognized here are to raise the redox potential of MMOH and to make the successive transfer of two electrons the favored course. In addition, the studies presented here and in a previous report (Liu, Y., et al., 1995) suggest that both components enhance the catalytic efficiency by specifically modulating the rates of reactions in the course of the catalytic cycle. It seems reasonable that these roles of MMOB and MMOR are aspects of a regulatory mechanism of MMO designed to allow efficient electron transfer and oxygen activation while maintaining tight coupling of energy utilization with substrate oxidation. Our current understanding of this regulatory system, summarized in Figure 8, suggests that it differs in some fundamental respects from those of other well-studied enzymes in the oxygenase family.

One interpretation of the kinetic observations made thus far is that resting MMOH in the absence of MMOB and MMOR exists in a conformation which in some manner "hinders"[4] access to the active site (Figure 8, inner circle, pentagons). This proposal is in accord with (i) the X-ray crystal structures of MMOH from *M. capsulatus* and *M. trichosporium*, which show no direct passage for the substrate into the diiron cluster (Rosenzweig et al., 1993, 1995; Elango et al., 1997), (ii) our observation that O_2 reacts slowly with the diiron cluster in the diferrous state (Liu, Y., et al., 1995), and (iii) our observations that the diiron cluster interacts very slowly with phenol (a product that binds to the diiron cluster) in the diferric state (Andersson et al., 1992). Thus, catalysis will not be efficient because the reaction with O_2 in this state is very slow. Hydrogen peroxide is known to react with the diferric state of MMOH, but the proposed limited access to the active site would present a barrier to this reagent, perhaps accounting for the high K_M value for turnover (~250 mM) (Andersson et al., 1991).

Two seemingly opposing effects of the formation of the MMOH−MMOB complex are to increase the rate of reaction of diferrous MMOH with O_2 (Liu, Y., et al., 1995) and decrease the rate of the reaction of diferric MMOH with peroxide (Froland et al., 1992). Consequently, it is proposed in Figure 8 (middle circle, octagons) that formation of the MMOH−MMOB complex will cause a redox sensitive structural change. The effects on the peroxide shunt suggest that this conformation of MMOH has an even more hindered active site structure in the diferric state, perhaps due to MMOB binding near the active site as suggested by the crystal structure (Rosenzweig et al., 1993, 1995; Elango et al., 1997). However, upon reduction, the active site appears to become more accessible, thereby facilitating reaction with O_2. The low redox potential of this species will also favor the oxidation of diferrous MMOH to facilitate O−O binding and bond breaking. Thus, catalysis should be efficient once the transfer of two electrons to MMOH is accomplished, which is in agreement with the observation of our single-turnover studies that the product formation rate is much faster and more efficient when MMOH is complexed with MMOB (Liu, Y., et al., 1995). However, the actual transfer of electrons from any potential donor will be inhibited by the fact that the potential is low and the relative magnitudes of the individual potentials of the cluster irons favor the transfer of one rather than two electrons as required for catalysis. After reaction with O_2, the formation of compounds P and Q proceeds rapidly. The accessibility of the active site is also strongly implied by the second-order kinetic nature of the reaction of compound Q with substrates (Lee et al., 1993b; Nesheim & Lipscomb, 1996), suggesting an essentially collisional reaction.

In the presence of MMOR, the K_M value for H_2O_2 in the peroxide shunt is similar to that observed for MMOH alone, but the inhibitory effect of MMOB is not observed as shown in the studies presented here. Also, significant changes in the redox potential and product yield characteristics of MMOH occur when it interacts with MMOR. Thus, it is proposed that a third conformation (Figure 8, outer circle,

[3] The ratio of components in the cell free extract is approximately MMOH:MMOB:MMOR = 1:1:0.1 (sites) based on the specific activities of the purified components.

[4] The interactions of MMOH with O_2, H_2O_2, and substrates appear to be either "hindered" or "facilitated" in the various component complexes and MMOH redox states. It is unclear whether this results from the active site physically closing and opening, alterations in the ligation of the diiron cluster, or changes in the reactivity of the cluster due to changes in redox potential. In the discussion presented here, we will limit our interpretations to the general concept of accessibility recognizing the physical basis for this remains undefined.

circles) occurs which also has a relatively closed active site structure in the diferric state. This conformation is able to bind reduced MMOR to accept two electrons and assume an open structure which allows relatively rapid reaction with O_2. The results presented here suggest that the new configuration induced by interaction with MMOR appears to also increase the rate of conversion of compound P to compound Q, thereby potentially diminishing a competing nonproductive autodecay of compound P and increasing the product yield as observed. In general, the structural characteristics that dictate the substrate accessibility of this conformation are determined by the MMOH−MMOB interaction because MMOR binding by itself will not stimulate the oxygen reactivity of diferrous MMOH. However, the structural changes associated with the MMOH−MMOR interaction do enforce a high overall redox potential, redox potentials that favor two electron reduction of MMOH, and alterations in the reaction cycle kinetics that enhance the catalytic efficiency of the system. Although the MMOR is apparently present in the cell in only about 10% of the MMOH concentration (Fox et al., 1989) the results presented here suggest that the hysteresis in the putative MMOH′ structure upon dissociation of MMOR would preserve this favorable conformation long enough for catalysis to proceed.

For the MMO system, as well as all other oxygenase enzymes, it is important to prevent the generation of diffusable reactive species, as well as to couple reducing equivalent utilization tightly to substrate oxidation. In the scheme proposed, these regulatory requirements are accommodated through efficient transfer of two electrons linked to rapid reaction with O_2, an increased accessibility to substrates, decreased accumulation of compound P that may release reactive species without substrate hydroxylation, and possibly adoption of a conformation that prevents futile transfer of electrons from MMOR to the high-valent species, compound Q. All of these facets of MMO regulation are different from the substrate dependent redox potential switching and component specific electron transport (Sligar et al., 1974; Sligar & Gunsalus, 1976; Lipscomb et al., 1976) which characterize the regulatory system envisioned for enzymes such as cytochrome P450.

REFERENCES

Aasa, R., & Vänngård, T. (1975) *J. Magn. Reson. 19*, 308−315.

Andersson, K. K., Froland, W. A., Lee, S.-K., & Lipscomb, J. D. (1991) *New J. Chem. 15*, 411−415.

Andersson, K. K., Elgren, T. E., Que, L., Jr., & Lipscomb, J. D. (1992) *J. Am. Chem. Soc. 114*, 8711−8713.

Dalton, H. (1980) *Adv. Appl. Microbiol. 26*, 71−87.

DeWitt, J. G., Rosenzweig, A. C., Salifoglou, A., Hedman, B., Lippard, S. J., & Hodgson, K. O. (1995) *Inorg. Chem. 34*, 2505−2515.

Elango, N., Radhakrishman, R., Froland, W. A., Wallar, B. J., Earhart, C. A., Lipscomb, J. D., & Ohlendorf, D. H. (1997) *Protein Sci. 6*, 556−568.

Fee, J. A. (1978) *Methods Enzymol. 49*, 512−528.

Fogg, P. G. T., & Gerrard, W. (1991) in *Solubility of Gases in Liquids*, p 166, John Wiley and Sons, New York.

Fox, B. G., Surerus, K. K., Münck, E., & Lipscomb, J. D. (1988) *J. Biol. Chem. 263*, 10553−10556.

Fox, B. G., Froland, W. A., Dege, J. E., & Lipscomb, J. D. (1989) *J. Biol. Chem. 264*, 10023−10033.

Fox, B. G., Borneman, J. G., Wackett, L. P., & Lipscomb, J. D. (1990a) *Biochemistry 29*, 6419−6427.

Fox, B. G., Froland, W. A., Jollie, D. R., & Lipscomb, J. D. (1990b) *Methods Enzymol. 188*, 191−202.

Fox, B. G., Liu, Y., Dege, J. E., & Lipscomb, J. D. (1991) *J. Biol. Chem. 266*, 540−550.

Fox, B. G., Hendrich, M. P., Surerus, K. K., Andersson, K. K., Froland, W. A., & Lipscomb, J. D. (1993) *J. Am. Chem. Soc. 115*, 3688−3701.

Froland, W. A., Andersson, K. K., Lee, S. K., Liu, Y., & Lipscomb, J. D. (1992) *J. Biol. Chem. 267*, 17588−17597.

Hendrich, M. P., Münck, E., Fox, B. G., & Lipscomb, J. D. (1990) *J. Am. Chem. Soc. 112*, 5861−5865.

Hendrich, M. P., Fox, B. G., Andersson, K. K., Debrunner, P. G., & Lipscomb, J. D. (1992) *J. Biol. Chem. 267*, 261−269.

Lee, S.-K., Fox, B. G., Froland, W. A., Lipscomb, J. D., & Münck, E. (1993a) *J. Am. Chem. Soc. 115*, 6450−6451.

Lee, S.-K., Nesheim, J. C., & Lipscomb, J. D. (1993b) *J. Biol. Chem. 268*, 21569−21577.

Lipscomb, J. D. (1994) *Annu. Rev. Microbiol. 48*, 371−399.

Lipscomb, J. D., Sligar, S. G., Namtvedt, M. J., & Gunsalus, I. C. (1976) *J. Biol. Chem. 251*, 1116−1124.

Liu, K. E., & Lippard, S. J. (1991) *J. Biol. Chem. 266*, 12836−12839.

Liu, K. E, & Lippard, S. J. (1995) *Adv. Inorg. Chem. 42*, 263−289.

Liu, K. E., Valentine, A. M., Qiu, D., Edmondson, D. E., Appelman, E. H., Spiro, T. G., & Lippard, S. J. (1995a) *J. Am. Chem. Soc. 117*, 4997−4998.

Liu, K. E., Valentine, A. M., Wang, D. L., Huynh, B. H., Edmondson, D. E., Salifoglou, A., & Lippard, S. J. (1995b) *J. Am. Chem. Soc. 117*, 10174−10185.

Liu, Y., Nesheim, J. C., Lee, S. K., & Lipscomb, J. D. (1995) *J. Biol. Chem. 270*, 24662−24665.

Lund, J., & Dalton, H. (1985) *Eur. J. Biochem. 147*, 291−296.

Nesheim, J. C., & Lipscomb, J. D. (1996) *Biochemistry 35*, 10240−10247.

Paulsen, K. E., Liu, Y., Fox, B. G., Lipscomb, J. D., Münck, E., & Stankovich, M. T. (1994) *Biochemistry 33*, 713−722.

Pulver, S., Froland, W. A., Fox, B. G., Lipscomb, J. D., & Solomon, E. I. (1993) *J. Am. Chem. Soc. 115*, 12409−12422.

Rosenzweig, A. C., Frederick, C. A., Lippard, S. J., & Nordlund, P. (1993) *Nature 366*, 537−543.

Rosenzweig, A. C., Nordlund, P., Takahara, P. M., Frederick, C. A., & Lippard, S. J. (1995) *Chem. Biol. 2*, 409−418.

Shu, L., Nesheim, J. C., Kauffmann, K., Münck, E., Lipscomb, J. D., & Que, L., Jr. (1997) *Science 275*, 515−518.

Sligar, S. G., & Gunsalus, I. C. (1976) *Proc. Natl. Acad. Sci. U.S.A. 73*, 1078−1082.

Sligar, S. G., Debrunner, P. G., Lipscomb, J. D., & Gunsalus, I. C. (1974) *Proc. Natl. Acad. Sci. U.S.A. 71*, 3906−3910.

Wallar, B. J., & Lipscomb, J. D. (1996) *Chem. Rev. 96*, 2625−2657.

BI962743W